Available online at www.sciencedirect.com
ScienceDirect
Journal of Sound and Vibration 325 (2009) 14–33
JOURNAL OF SOUND AND VIBRATION
www.elsevier.com/locate/jsvi

On the relationship between viscous and hysteretic damping models and the importance of correct interpretation for system identification

R.M. Lin*, J. Zhu

School of Mechanical and Aerospace Engineering, Nanyang Technological University, 50 Nanyang Avenue, Singapore 639798, Singapore

Received 22 January 2007; received in revised form 30 April 2008; accepted 28 February 2009
Handling Editor: L.G. Tham
Available online 2 April 2009

Abstract

In engineering practice, both viscous and hysteretic damping models are usually employed to characterize damped dynamic properties of linear mechanical systems, the identification of which has long been an active area of research in experimental modal analysis. This paper is devoted to investigate the relationship between viscous and hysteretic damping models. In order to show whether the arbitrary choice of damping model is reasonable, the relationship has been derived based on two normalization procedures and the modal parameter identification procedure. In case of proportional damping, there exists an exact relationship between hysteretic and viscous damping models as $\eta_r = 2\xi_r$. As for non-proportional damping, the equivalent mode shapes and their counterparts of the original system are almost the same except differing by a complex scaling factor. The numerical cases based on the simulated modal identification procedure have demonstrated that the error in the estimation of modal parameters caused by arbitrarily choosing damping model is quite small. Furthermore, the equivalent damping matrix is physically sensible in the case of the system with distributed damping whereas, no physically sensible equivalent damping matrix exists in the case where the damping is localized. The validity of the relationship between the two damping models has been further verified by a practical experimental example.

1. Introduction

In modern engineering practice, the quality of a vibration model of a mechanical system is essential for a wide range of applications as, for instance, the prediction of system dynamic behavior, damage detection and system design and optimization. Most mechanical systems exhibit damped dynamic behaviors, which may prevent the systems from being accurately identified since understanding of damping mechanisms is still quite primitive. Therefore, the estimation or identification of damping models is always the central topic in experimental modal analysis. By far the most common damping model employed in practice is the so-called 'proportional damping' or 'Rayleigh damping' introduced by Rayleigh [1], which is linear and supposed to be determined only by the instantaneous generalized velocity. And the damping matrix is assumed to be a linear

*Corresponding author. Tel.: +65 6790 4728; fax: +65 6791 1975.
E-mail address: mrmlin@ntu.edu.sg (R.M. Lin).

0022-460X/$ - see front matter
doi:10.1016/j.jsv.2009.02.051

combination of system's mass and stiffness matrices and hence real normal modes as those of the undamped case can be preserved. Caughey [2] presented the general conditions on the form of proportional damping matrix, under which a damped system processes classic real normal modes. A series expression for damping matrix in terms of mass and stiffness matrices was proposed by Caughey and O'Kelly [3] so that a damped system can be decoupled by real normal modes. And it was also shown that the Rayleigh damping is just a special case of this general expression. Since the proportional damping matrix can be diagonalized simultaneously with the mass and stiffness matrices using real normal modes, a proportionally damped system can be decoupled into a set of principal single-degree-of-freedom (sdof) systems. Based on the decoupled damped system, for majority modal analysis applications [4,5], general expression of frequency response function (FRF) in the form of real normal modes can be derived. Then the damping parameters can be easily estimated using measured FRFs and the modal damping matrix (viscous or hysteretic) can be established by using the normal mode theory.

However, most practical structural systems under modal testing possess general non-proportional damping and hence exhibit complex mode behavior. For a non-proportionally damped system, the equations of motion cannot be decoupled in the modal coordinates due to the non-diagonal nature of the modal damping matrix. And consequently the system possesses complex modes instead of real normal modes. From the viewpoint of mathematics, complex modes refer to the complex solution of the eigenproblem of a general damped system, which can be transformed into the vibrational characteristics of the system. For complex modes, each natural frequency and mode shape of the system is described in terms of complex quantities. In spite of lots of research efforts, understanding and identification of complex modes is not as well developed as those for real normal modes. To overcome the difficulties induced by the existence of complex modes in the identification of a mechanical system, real normal modes are usually required in experimental modal analysis. Ibrahim [6], Lin and Ibrahim [7] and Chen et al. [8] proposed methods to obtain the best real normal modes from identified complex modes. The extracted normal modes were then used to construct a proportional damping model together with modal damping matrix.

Since proportional damping is well understood and commonly accepted in the description of damped dynamic behavior of a system, identification of damping models for proportionally damped systems is required. Based on a generalized proportional damping model, Adhikari [9] presented a method for identification of damping matrix using experimental modal analysis in the case where the system to be identified is effectively proportionally damped and the modes almost complex. In view of identification of damping in time domain, Gaylard [10] presented an improved weighted matrix integral of system response functions to identify proportional damping model by introducing a state-space approach. However, damping identification using this method may lack uniqueness. On the other hand, a practical way for damping identification is to assume a proportional damping model for damped mechanical systems. Angeles and Ostrovskaya [11] proposed a method to extract proportional damping component of an arbitrary damping matrix, which approximates optimally the original damping matrix in the least-square sense. However, even results drawn from the best proportional-damping approximation can be practically misleading in most cases.

In 1990s, a large number of literatures were devoted to the investigation of non-proportional damping of a mechanical system [12–15], which still remains an issue in modal parameter estimation. A few effective methods have been developed to identify non-proportional damping matrix from experimentally measured complex modes in case of lightly damped structures [16–18]. Woodhouse [16] discussed linear damping models: the familiar dissipation-matrix model and the general linear model and presented simple expressions for complex modal data and transfer functions. Following this idea, Adhikari and Woodhouse [17] presented a first order perturbation method to obtain a full viscous (non-proportional) damping matrix from complex modal data in the case of sufficiently light damping. This method constructs the physical damping matrix using the inverse transformation of the modal damping matrix from the decoupling of the damped system. The two authors [18] further developed the first perturbation method to identify a non-viscous (non-proportional) damping model by using experimentally identified complex modal data together with the system mass matrix. Prells and Friswell [19] considered to determine symmetric non-proportional modal damping matrix using real normal modes and undamped natural frequencies based on a generalized modal model of a system. In this case the modal damping matrix is symmetric but non-diagonal due to non-proportional damping. Kasai and Link [20] presented a measure of non-proportional damping in terms of damping ratio based on the investigation of the difference between proportional and general viscous damping models.

To date, most proposed methods to identify or estimate damping no matter it is proportional or non-proportional [9–20] are based on a viscous damping model, whose mechanism is well understood. In fact, for simplicity in engineering calculation and analysis, both viscous damping and hysteretic damping models are generally adopted to describe damping properties in linear vibratory mechanical systems [4,5]. They are also the most often encountered damping types in practice. Although other damping models have been proposed from time to time, it has become common practice in modal analysis that either a hysteretic or viscous damping model can be readily used in the interpretation of measured vibration data. However, no verification has been made as to show whether or not this kind of arbitrary interpretation is physically reasonable. Due to the uncertainty of the type of damping model in practical complex structural systems, it is important to demonstrate theoretically whether this arbitrary choice of damping model will cause large errors in the estimation of modal parameters. Because these parameters are regarded as accurate ones once estimated and they are to be used with confidence to establish the system's mass and stiffness matrices or modify these matrices of the analytical model which are modeled using Finite Element Method. A large number of studies [6–20] have ignored this topic, which may have an effect on the identified results of the modal analysis for a damped system. The primary research work on the issue was conducted by Balmés in Ref. [21], where an identification procedure was proposed to extract the normal modes from the experimental complex modes. Meanwhile, the relation between normal modes (hysteretic damping case) and complex modes (viscous damping case) was investigated in details. It was found that the normal modes are clearly associated with the complex modes in terms of modal damping model and eigenvectors in the case of a proportionally damped system. In fact, for the general mechanical systems with same mass and stiffness matrices and different damping properties (such as viscous damping or hysteretic damping), there may exist a relationship between the modal models of these two systems since they have the similar FRF models, which may also represent systems' dynamic characteristics in nature. If this relationship can be shown, it may help us to understand the difference between the same systems with various damping models and choose a suitable damping model for a mechanical system when modal analysis is performed.

In this paper, the authors address the relationship between viscous and hysteretic damping models in proportional case and general non-proportional case. Based on the identified results of seven simulated numerical examples and an experimental test, this paper shows that the error for the estimation of modal parameters due to the wrong interpretation of damping model (data from viscous damping model have been interpreted as hysteretic one or vice versa) is really very small. And in the case that the damping is distributed, for either types of damping, there exists a physically sensible (positive-definite or semi-positive definite) equivalent damping matrix on the basis that these two systems (in fact, only the damping matrix is different) have the same response model. On the other hand, however, if the damping is localized in the system, the correct interpretation of damping model becomes greatly important. Because if the mathematical model of damping is sought (damping matrix of the system), in this case there are no physically sensible equivalent damping matrices on that basis.

2. Mass normalization and 'A' normalization

The modal model of a system consists of eigenvalue matrix $[\omega_r^2]$ and eigenvector matrix $[\Psi]$, where the eigenvalue matrix is unique while the eigenvector matrix is not. The non-unique eigenvectors or mode shapes are subject to an arbitrary scaling factor which does not affect the shape of the vibration mode, but only its amplitude. The procedure of scaling the eigenvectors is called 'normalization', which is largely governed by the numerical procedures followed by the eigensolution of a dynamic system. In experimental modal analysis, there exist two standard mode shape normalization procedures based on the two different damping models. One is called 'Mass Normalization' (normalized to the system's mass matrix $[M]$) which is for the case of hysteretic damping and the other is called 'A Normalization' (normalized to the system's generalized mass matrix $[A]$) which is used for viscous damping [22]. In order to investigate the relationship between viscous and hysteretic damping models, the various eigensolutions of the systems in the case of two different damping models, which correspond to the two normalization procedures, respectively, need to be introduced firstly.

For a multi-degree-of-freedom (mdof) system with general viscous damping, the generalized eigenvalue problem of the system can be written as,

$$([A]s_r + [B])\{\theta\}_r = \{0\}; \quad r = 1, 2n, \tag{1}$$

where s_r and $\{\theta\}_r$ are the $2n$ eigenvalues and eigenvectors of the system. $[A]$ and $[B]$ are system's generalized mass and stiffness matrices which have the forms, respectively, as,

$$[A] = \begin{bmatrix} [C] & [M] \\ [M] & [0] \end{bmatrix} \quad \text{and} \quad [B] = \begin{bmatrix} [K] & [0] \\ [0] & -[M] \end{bmatrix}. \tag{2}$$

By solving Eq. (1), the eigenvalues and the so-called 'A normalized' eigenvectors, which are normalized to the generalized mass matrix $[A]$, can be obtained in terms of matrix form as, respectively,

$$[S] = \begin{bmatrix} [\Lambda] & [0] \\ [0] & [\Lambda]^* \end{bmatrix} \quad \text{and} \quad [\Theta] = \begin{bmatrix} [\Psi] & [\Psi]^* \\ [\Psi][\Lambda] & [\Psi]^*[\Lambda]^* \end{bmatrix}. \tag{3}$$

Here, $[\Lambda]$ is the diagonal matrix of complex eigenvalues, which can be expressed as,

$$[\Lambda] = [s_r], \quad s_r = \omega_r(-\xi_r + \mathrm{i}\sqrt{1-\xi_r^2}), \quad (r = 1, 2, \ldots, n). \tag{4}$$

From Eq. (3), it is obvious that the eigenproperties of the viscously damped system will be in general complex and always occur in conjugate pairs. Hence, the orthogonality properties of the eigensolution are stated as,

$$[\Theta]^{\mathrm{T}}[A][\Theta] = [I] \quad \text{and} \quad [\Theta]^{\mathrm{T}}[B][\Theta] = [S]. \tag{5}$$

The eigenvalue problem for an mdof system in the case of hysteretic damping can be expressed as,

$$(-\lambda_r^2[M] + [K] + \mathrm{i}[D])\{\phi\}_r = \{0\}; \quad r = 1, n. \tag{6}$$

Solving the above eigenproblem leads to the solution containing complex eigenvalues λ_r^2 and eigenvectors $\{\phi\}_r$. The eigensolution of Eq. (6) is standard when compared with that of Eq. (1) and since $[A] \equiv [M]$ and $[B] \equiv [K] + \mathrm{i}[D]$ in this case, the eigenvectors for the hysteretic damping case are therefore mass-normalized (normalized to the mass matrix $[M]$ of the system). The eigensolution possesses the orthogonality properties, which are defined by the equations,

$$[\Phi]^{\mathrm{T}}[M][\Phi] = [I] \quad \text{and} \quad [\Phi]^{\mathrm{T}}[K + \mathrm{i}D][\Phi] = [\lambda_r^2], \tag{7}$$

where $[\Phi]$ is the mass-normalized eigenvector matrix and $[\lambda_r^2]$ is the diagonal matrix of complex eigenvalues.

The eigenvalues of the damped system from Eqs. (1) and (6) are obviously different and hence the study is focused on the eigenvectors of the damped system for various damping models. Since different normalization procedures are used in the eigenproblems for the case of viscous and hysteretic damping models, respectively, the corresponding mode shapes (eigenvectors) are visually quite different even for the case of a proportionally damped system. The differences in amplitudes as well as phase angles of the corresponding eigenvectors often cause confusion to analysts. And it is therefore necessary to establish the relationship between the 'A-normalized' and mass-normalized eigenvectors. In fact, the mode shapes for the case of viscous and hysteretic damping models differ simply by a complex scaling factor, which will be shown by the later derivation. However, according to modal testing theory [4], if the damping is proportional, no matter what type of damping model is used, the mode shapes are expected to be exactly the same as those of the corresponding undamped system. So what is the relationship between these two sets of mode shapes when the damping is proportional? In other words, what is the scaling factor for each mode between the two proportionally damped systems? In the case of proportional damping, suppose the Mass Normalized mode shape matrix $[\Phi]_{n\times n}$ and the 'A' Normalized mode shape matrix $[\Psi]_{n\times n}$ have the relationship as $[\Psi]_{n\times n} = [\Phi]_{n\times n}[N]_{n\times n}$, where $[N]_{n\times n}$ is a diagonal matrix of complex coefficients. Then the relationship between the mode shape matrices in case of different damping models is to determine the coefficient matrix $[N]$, which can be derived as follows. For a general viscously damped system, the orthogonality properties of the modal model can be expressed as, if the complex conjugate of the eigenvalues and eigenvectors are not considered,

$$\begin{bmatrix} [\Psi] \\ [\Psi][\Lambda] \end{bmatrix}^{\mathrm{T}}_{n\times 2n} \begin{bmatrix} [C] & [M] \\ [M] & [0] \end{bmatrix}_{2n\times 2n} \begin{bmatrix} [\Psi] \\ [\Psi][\Lambda] \end{bmatrix}_{2n\times n} = [I]_{n\times n}. \tag{8}$$

Expanding the left side of Eq. (8), we have the following equation,

$$[\Psi]^{\mathrm{T}}[C][\Psi] + [\Lambda]^{\mathrm{T}}[\Psi]^{\mathrm{T}}[M][\Psi] + [\Psi]^{\mathrm{T}}[M][\Psi][\Lambda] = [I]. \tag{9}$$

Substituting $[\Psi] = [\Phi][N]$ into Eq. (9), we can have,

$$[N]^{\mathrm{T}}[\Phi]^{\mathrm{T}}[C][\Phi][N] + [\Lambda]^{\mathrm{T}}[N]^{\mathrm{T}}[\Phi]^{\mathrm{T}}[M][\Phi][N] + [N]^{\mathrm{T}}[\Phi]^{\mathrm{T}}[M][\Phi][N][\Lambda] = [I]. \tag{10}$$

The orthogonality of the proportionally and viscously damped system is as follows,

$$[\Phi]^{\mathrm{T}}[M][\Phi] = [I] \quad \text{and} \quad [\Phi]^{\mathrm{T}}[C][\Phi] = [2\xi_r\omega_r], \tag{11}$$

where $[2\xi_r\omega_r]$ is a diagonal matrix. Then, based on Eq. (11), Eq. (10) can be simplified to the following equation,

$$[N]^{\mathrm{T}}[2\xi_r\omega_r][N] + [\Lambda]^{\mathrm{T}}[N]^{\mathrm{T}}[N] + [N]^{\mathrm{T}}[N][\Lambda] = [I]. \tag{12}$$

Since both $[2\xi_r\omega_r]$ and $[\Lambda]$ are diagonal matrices, we can rewrite above equation as,

$$(2[\xi_r\omega_r] + 2[\Lambda])[N]^2 = [I]. \tag{13}$$

Upon substituting Eq. (4) into Eq. (13) and solving it, we derive the expression for $[N]$ as,

$$[N]^2 = [(1/(2\mathrm{i}\omega_r\sqrt{1-\xi_r^2}))]. \tag{14}$$

As $[N]$ is a diagonal matrix of coefficients, from Eq. (14), the diagonal elements in the matrix can be determined easily as,

$$N_r = \mathrm{e}^{-\mathrm{i}\pi/4}\Big/\sqrt{2\omega_r\sqrt{1-\xi_r^2}} \quad (r = 1, \ldots, n). \tag{15}$$

From Eq. (15), it is clear that for a proportionally damped system, the 'A' Normalized eigenvector of the rth mode is simply the corresponding Mass Normalized eigenvector scaled by a factor of $1\Big/\sqrt{2\omega_r\sqrt{1-\xi_r^2}}$ and a phase angle rotation of $\pi/4$. Therefore, the modal models of a proportionally damped system should be considered to be similar for different damping models since there is only a complex scaling factor between each mode shape for two mode shape matrices.

3. The relationship between viscous and hysteretic damping models

As mentioned above, when the damping of a system is proportional, the mode shapes are the same as those of the corresponding undamped system no matter the system is viscously damped or hysteretically damped. As for other modal parameters, the undamped natural frequencies are the same because these two systems have the same mass matrix and stiffness matrix. And damping loss factor η_r for hysteretic case and damping ratio ξ_r for viscous case have a simple relationship as $\eta_r = 2\xi_r$, which can be derived from the similar FRF models of viscous case and hysteretic case. Furthermore, if a proportional viscously damped (or hysteretically damped) system is given, by performing modal analysis on it's FRF model, the system's mass matrix $[M]$, stiffness matrix $[K]$ and damping matrix $[D]$ (or $[C]$) are derived based on hysteretic (or viscous) damping assumption. Then, the system's matrices $[M]$ and $[K]$ are exactly the same as those of the original system and the equivalent damping matrix $[D]$ (or $[C]$) is different from the original damping matrix. Although it is not proportional (i.e. cannot be expressed by linear combination of $[M]$ and $[K]$), with this damping matrix, the system's mode shapes are still real. However, for a non-proportionally damped system, the relationship between these two sets of modal parameters is no longer so simple and cannot be readily derived. Because, in this case the real normal modes cannot be preserved due to the un-decoupling nature of the non-proportional damping. In order to establish the relationship, the receptance FRF in the case of viscous damping is first presented, which can be written as [4],

$$\alpha(\omega) = \sum_{r=1}^{n} \frac{(A_r + \mathrm{i}(\omega/\omega_r)B_r)}{(\omega_r^2 - \omega^2 + 2\mathrm{i}\omega\omega_r\xi_r)}. \tag{16}$$

Here, some approximation has to be made in order to carry out the sdof modal analysis. That is, in the vicinity of the rth resonance, a FRF is dominated by the rth mode so that the receptance expression for the viscous damping case is approximately written as,

$$\alpha(\omega) \approx \frac{(A_r + \mathrm{i}(\omega/\omega_r)B_r)}{(\omega_r^2 - \omega^2 + 2\mathrm{i}\omega\omega_r\xi_r)}, \tag{17}$$

where A_r and B_r are the real and imaginary parts of modal constant, respectively. Since the ratio between sweeping frequency and natural frequency is close to 1 at the rth resonance range (i.e., $\omega/\omega_r \cong 1$), the above equation can be further approximated as,

$$\alpha(\omega)|_{\omega \cong \omega_r} = \frac{(A_r + \mathrm{i}B_r)}{(\omega_r^2 - \omega^2 + 2\mathrm{i}\omega_r^2\xi_r)}. \tag{18}$$

During practical modal analysis procedure, the difference between modal parameters of a viscously damped system obtained using Eqs. (18) and (17) is really quite small. It is usually within the analysis error if the damping ratio is less than 4%. The receptance FRF for the hysteretic damping case has the same form as Eq. (18), provided that $\eta_r = 2\xi_r$, which can be written as,

$$\alpha(\omega) = \frac{(A_r + \mathrm{i}B_r)}{(\omega_r^2 - \omega^2 + \mathrm{i}\omega_r^2\eta_r)}. \tag{19}$$

Eqs. (18) and (19) are equations from which the relationship between these two eigenvector matrices in different damping cases can be established based on the assumption that these two systems have the same frequency response model around resonance. Also Eqs. (18) and (19) show that during the modal parameters identification stage, either Eq. (18) or (19) can be chosen for modal analysis no matter viscous damping case or hysteretic damping case.

To investigate the relation of these two damping models for non-proportional case, the modal identification procedure, where the damping model is arbitrarily chosen for a damped system, should be illustrated briefly. Generally, the curve-fitting identification method, which includes Circle-fit method and Line-fit method, is widely used in order to extract modal parameters from measured FRFs. These two methods are established for the case of hysteretically damped systems. The theory and typical procedures of the methods can be referred to [4]. Based on these identification methods, the whole process of modal parameter identification for a damped system (if one damping model is interpreted as another model) can be illustrated as follows (for two cases):

1. From viscous damping model to hysteretic damping model (i.e. deriving a hysteretically damped system to have the same response model around resonances as the original viscously damped one):
   (a) Measure the FRFs of the system with viscous damping (one row or column of receptance matrix).
   (b) Analyze these FRFs to obtain modal parameters (ω_r, η_r or ξ_r, A_r and B_r) based on the receptance form of Eq. (19) using modal analysis method.
   (c) Interpret these modal parameters as those from hysteretic damping model to obtain mode shape matrix.
   (d) Use this mode shape matrix to derive the system's mass, stiffness and equivalent hysteretic damping matrices.
2. From hysteretic damping model to viscous damping model, the similar procedure of modal parameter identification can be followed. The only different step is step (c), where the modal parameters are interpreted as those from viscous damping model to obtain mode shape matrix.

The theory of relationship between various eigenvector matrices behind this practice is shown as follows. Suppose all the elements of the modal constant vector, A_{jr} and B_{jr} ($j = 1, \ldots, n$), for the rth mode have been derived using modal analysis. Then if a hysteretic damping model is employed to interpret them, the mode shape for the rth mode has the form $\Phi_{jr} = (A_{jr} + \mathrm{i}B_{jr})/\sqrt{A_{rr} + \mathrm{i}B_{rr}}$, $(j = 1, \ldots, n)$, where A_{rr} and B_{rr} are real and imaginary parts of the diagonal elements of the modal constant matrix, respectively. If, on the other hand, a viscous damping model is chosen to interpret them, the mode shape for the rth mode is $\Psi_{jr} = G_{jr}/\sqrt{G_{rr}}$, $(j = 1, \ldots, n)$ and G_{jr} is related to A_{jr} and B_{jr} by the following equation:

$$G_{jr} = \frac{B_{jr}}{2\omega_r} + \frac{\mathrm{i}(-A_{jr} + \xi B_{jr})}{2\omega_r\sqrt{1 - \xi_r^2}}. \tag{20}$$

If we write $A_{jr} + \mathrm{i}B_{jr} = A_m \mathrm{e}^{\mathrm{i}\theta}$ and $G_{jr} = G_m \mathrm{e}^{\mathrm{i}\varphi}$, then from Eq. (20), the following relationship can be derived,

$$A_m = G_m(2\omega_r\sqrt{1 + \xi_r^2 \cos 2\varphi - \xi_r\sqrt{1 - \xi_r^2}\sin 2\varphi}), \tag{21}$$

and

$$\operatorname{ctg}\theta = \xi_r - \sqrt{1 - \xi_r^2}\operatorname{tg}\varphi. \tag{22}$$

From Eq. (21), since the maximum value for $\xi_r^2 \cos 2\varphi - \xi_r\sqrt{1 - \xi_r^2}\sin 2\varphi$ is $\sqrt{(\xi_r^2)^2 + (\xi_r\sqrt{1 - \xi_r^2})^2} = \xi_r$ and the value of ξ_r is usually small (<0.05), A_m is effectively equal to $2\omega_r G_m$ (the percentage error for this estimation, if we take the Taylor series expansion of $\sqrt{1 + \xi_r}$, is at the level of ξ_r^2). Suppose that the rth mode shapes for the case of hysteretic and viscous damping models can be rewritten as, respectively,

$$\Phi_{jr} = A_m^{jr}\mathrm{e}^{\mathrm{i}\theta_{jr}}/\sqrt{A_m^{rr}\mathrm{e}^{\mathrm{i}\theta_{rr}}} = A_m^{jr}\mathrm{e}^{\mathrm{i}(\theta_{jr} - \theta_{rr}/2)}/\sqrt{A_m^{rr}}, \tag{23}$$

$$\Psi_{jr} = G_m^{jr}\mathrm{e}^{\mathrm{i}\varphi_{jr}}/\sqrt{G_m^{rr}\mathrm{e}^{\mathrm{i}\varphi_{rr}}} = G_m^{jr}\mathrm{e}^{\mathrm{i}(\varphi_{jr} - \varphi_{rr}/2)}/\sqrt{G_m^{rr}}. \tag{24}$$

then it can be found that the moduli of the rth mode shape for the viscous case is the corresponding moduli of the rth mode shape for the hysteretic case scaled by a constant which is equal to $1/\sqrt{2\omega_r}$. As for Eq. (22), although it is difficult to prove it mathematically, the maximum error for the estimation of $\theta = \varphi - \pi/2$ or $\theta = \varphi + \pi/2$ is less than 4° if the damping ratio is less than 5% (this can be illustrated by examples given in the following section). Base on the above approximate relationship $\theta = \varphi - \pi/2$ (or $\theta = \varphi + 3\pi/2$), from Eqs. (23) and (24), it can be derived that the rth mode shape for the viscous damping case is the rth mode shape for the hysteretic damping case rotated by a constant phase angle which is -45° or 135° (or -225°) since the phase difference between two mode shapes is equal to $\theta_{jr} - \varphi_{jr} - (\theta_{rr} - \varphi_{rr})/2$. This has been proved by the following numerical cases. Combining these two features, it is clear that these two sets of mode shapes are roughly the same and this is what we expect because they are from the same system in the sense that the systems have the same response model.

4. The derivation of system matrices

Once modal parameters have been identified from the measured FRFs using modal analysis methods, the system's spatial model including mass, stiffness and damping matrices can be constructed using these parameters. In this section, a program has been written to simulate the modal analysis process for the verification of what has been put forward above. Given system's matrices $[M]$, $[K]$ and $[C]$ or $[D]$ for a damped system, the first step is to solve the eigenproblem to obtain eigenvalues and eigenvectors of the system. Based on the calculated eigenvalues and eigenvectors, the simulated FRFs are obtained. Then, in the simulated modal analysis process, the modal constants are calculated and used to derive the equivalent eigenvector matrix of its counterpart system (hysteretic damping case if $[C]$ was used and viscous damping case if $[D]$ was used). And subsequently this equivalent mode shape (eigenvector) matrix is used to calculate back the system's matrices. In the last paragraph, it was shown how the equivalent mode shape matrix could be derived and here we suppose that this mode shape matrix has already been obtained. Base on the calculated mode shape matrix, the system's matrices can be determined as follows for two cases:

1. *From viscous damping model to hysteretic damping model case*: The system's mass and stiffness matrices can be calculated as, respectively,

$$[M] = ([\Phi]^{\mathrm{T}})^{-1}[\Phi]^{-1}, \tag{25}$$

$$[K] + \mathrm{i}[D] = ([\Phi]^{\mathrm{T}})^{-1}[\omega_r^2(1 + \mathrm{i}\eta_r)][\Phi]^{-1}. \tag{26}$$

The damping matrix $[D]$ can be obtained by taking the imaginary part of the right side of Eq. (26).

2. *From hysteretic damping model to viscous damping model case*: Based on the eigenvalue and eigenvector matrices of the viscously damped system in Eq. (3), the generalized mass and stiffness matrices are determined as,

$$[A] = ([\Theta]^{\mathrm{T}})^{-1}[\Theta]^{-1}, \tag{27}$$

$$[B] = ([\Theta]^{\mathrm{T}})^{-1}[S][\Theta]^{-1}. \tag{28}$$

In this case, the calculated generalized stiffness matrix has the form,

$$[B] = \begin{bmatrix} -[K] & [0] \\ [0] & [M] \end{bmatrix}. \tag{29}$$

From the expressions of the generalized mass matrix $[A]$ in Eq. (2) and the generalized stiffness matrix $[B]$ in Eq. (29), the system's mass matrix $[M]$, stiffness matrix $[K]$ and damping matrix $[C]$ can be obtained by taking the partition matrices of $[A]$ and $[B]$, respectively.

5. Discussion of numerical case studies

In order to demonstrate the relationship between viscous and hysteretic damping models derived previously, seven numerical cases have been simulated and studied. In each case, a typical mechanical system consisting of mass–spring elements is presented, whose mass, stiffness and damping matrices are specified. Following the identification process in Section 3, the equivalent eigenvalue and eigenvector matrices of the system are calculated based on the improper interpretation of damping model. Consequently, the equivalent system's matrices are derived based on the identified modal data.

Case No. 1: A 3-dofs mass–spring system with proportional hysteretic damping is shown in Fig. 1. The following parameters are used for this system: $m_1 = 0.5\,\mathrm{kg}$, $m_2 = 1.0\,\mathrm{kg}$, $m_3 = 1.5\,\mathrm{kg}$; $k_1 = k_2 = k_3 = k_4 = k_5 = k_6 = 1000.0\,\mathrm{N/m}$; $d_j = 0.05k_j$, $j = 1, \ldots, 6$. In this hystereticly damped system, the damping model, which is distributed, is interpreted as a viscous damping model.

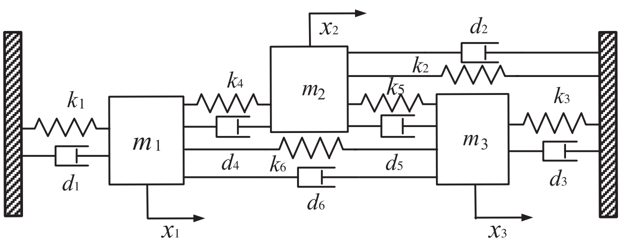

Fig. 1. A 3-dofs mass–spring model.

The original system's mass, stiffness and damping matrices in hysteretic damping case are obtained from the parameters as:

$$[M] = \begin{bmatrix} 0.5 & 0.0 & 0.0 \\ 0.0 & 1.0 & 0.0 \\ 0.0 & 0.0 & 1.5 \end{bmatrix}, \quad [K] = \begin{bmatrix} 3000 & -1000 & -1000 \\ -1000 & 3000 & -1000 \\ -1000 & -1000 & 3000 \end{bmatrix} \quad \text{and} \quad [D] = \begin{bmatrix} 150 & -50 & -50 \\ -50 & 150 & -50 \\ -50 & -50 & 150 \end{bmatrix}.$$

The mode shape matrix of this original system is given by the eigensolution of the system as:

$$[\Phi] = \begin{bmatrix} 0.464 & 0.218 & 1.318 \\ 0.536 & 0.782 & 0.318 \\ 0.635 & 0.493 & 0.142 \end{bmatrix}.$$

Following the modal identification process in Section 3, the eigenvalue and eigenvector matrices can be obtained and then the generalized mass matrix $[A]$ and stiffness matrix $[B]$ are calculated:

$$[A] = \begin{bmatrix} 1.895 & -0.419 & -0.467 & 0.500 & 0.000 & 0.000 \\ -0.419 & 2.628 & -0.610 & 0.000 & 1.000 & 0.000 \\ -0.467 & -0.610 & 3.169 & 0.000 & 0.000 & 1.500 \\ 0.500 & 0.000 & 0.000 & 0.000 & 0.000 & 0.000 \\ 0.000 & 1.000 & 0.000 & 0.000 & 0.000 & 0.000 \\ 0.000 & 0.000 & 1.500 & 0.000 & 0.000 & 0.000 \end{bmatrix},$$

and

$$[B] = \begin{bmatrix} -2999.1 & 1000 & 1000 & 0.0 & 0.0 & 0.0 \\ 1000 & -3000 & 1000 & 0.0 & 0.0 & 0.0 \\ 1000 & 1000 & -2999.1 & 0.0 & 0.0 & 0.0 \\ 0.0 & 0.0 & 0.0 & 0.5 & 0.0 & 0.0 \\ 0.0 & 0.0 & 0.0 & 0.0 & 1.0 & 0.0 \\ 0.0 & 0.0 & 0.0 & 0.0 & 0.0 & 1.5 \end{bmatrix}.$$

From the partition matrices of the above matrices $[A]$ and $[B]$, the equivalent mass, stiffness and damping matrices can be obtained, respectively. As can be seen, in this case the derived mass and stiffness matrices are same as those from the original system while the damping matrix is different from that of the hystereticly damped system. The equivalent mode shape matrix is calculated as:

$$[\Psi] = \begin{bmatrix} 0.059(-45^\circ) & 0.020(-45^\circ) & 0.103(-45^\circ) \\ 0.068(-45^\circ) & 0.072(-45^\circ) & 0.025(135^\circ) \\ 0.081(-45^\circ) & 0.046(-35^\circ) & 0.011(135^\circ) \end{bmatrix}.$$

Pre- and post- multiplying the damping matrix by the eigenvector matrix has the following condition,

$$[\Psi]^H[C][\Psi] = [\Psi]^H \begin{bmatrix} 1.895 & -0.419 & -0.467 \\ -0.419 & 2.627 & -0.610 \\ -0.467 & -0.610 & 3.168 \end{bmatrix} [\Psi] = \begin{bmatrix} 0.025 & 0 & 0 \\ 0 & 0.025 & 0 \\ 0 & 0 & 0.025 \end{bmatrix}.$$

From the above orthogonal properties of the damping matrix, it can be proved the obtained equivalent damping matrix from $[A]$ is physically sensible.

Case No. 2: In a similar 3-dofs mass–spring but separated system, which is non-proportionally and hystereticly damped, the damping model is interpreted as a viscous damping model. The system's mass and stiffness matrices are the same as those in Case No. 1. And the localized hysteretic damping matrix is:

$$[D] = \begin{bmatrix} 300 & 0 & 0 \\ 0 & 0 & 0 \\ 0 & 0 & 0 \end{bmatrix}.$$

The mode shape matrix of this original system can be obtained by solving the eigenproblem of the system as:

$$[\Phi] = \begin{bmatrix} 1.321(0.87^\circ) & 0.463(-5.54^\circ) & 0.217(172.6^\circ) \\ 0.316(173.3^\circ) & 0.537(0.02^\circ) & 0.784(178.9^\circ) \\ 0.142(176.9^\circ) & 0.636(0.96^\circ) & 0.492(-1.34^\circ) \end{bmatrix}.$$

The generalized matrices $[A]$ and $[B]$ are calculated:

$$[A] = \begin{bmatrix} 3.499 & -0.225 & 0.143 & 0.502 & 0.003 & 0.001 \\ -0.222 & 0.797 & 0.825 & 0.001 & 0.998 & -0.001 \\ 0.143 & 0.825 & 1.339 & -0.000 & -0.000 & 1.501 \\ 0.502 & 0.001 & -0.000 & 0.000 & 0.000 & 0.000 \\ 0.003 & 0.998 & -0.000 & 0.000 & -0.000 & -0.000 \\ 0.001 & -0.001 & 1.501 & 0.000 & -0.000 & -0.000 \end{bmatrix},$$

and

$$[B] = \begin{bmatrix} -3013 & 990 & 1000 & -0.857 & -1.956 & -2.251 \\ 990 & -2992 & 1003 & -0.223 & 0.781 & 0.808 \\ 1000 & 1003 & -3002 & 0.144 & 0.817 & 1.329 \\ -0.857 & -0.223 & 0.144 & 0.500 & 0.000 & -0.001 \\ -1.956 & 0.781 & 0.817 & 0.000 & 0.997 & -0.002 \\ -2.251 & 0.808 & 1.329 & -0.001 & -0.002 & 1.500 \end{bmatrix}.$$

The calculated equivalent eigenvector matrix is:

$$[\Psi] = \begin{bmatrix} 0.103(-44.1^\circ) & 0.059(-50.5^\circ) & 0.020(-52.4^\circ) \\ 0.025(128.3^\circ) & 0.068(-45.0^\circ) & 0.073(-43.9^\circ) \\ 0.011(131.9^\circ) & 0.081(-44.1^\circ) & 0.046(133.7^\circ) \end{bmatrix}.$$

In this case, the equivalent mass and stiffness matrices are almost same as those of the original system in hysteretic damping case, respectively. Compare the eigenvector matrices of the original and identified systems, it can be found that the moduli of the rth ($r = 1,2,3$) mode shape for viscous damping case are that for hysteretic damping case scaled by a constant (the constants are 0.127, 0.093 and 0.078 for the three modes, respectively), which is equal to $1/\sqrt{2\omega_r}$ ($r = 1,2,3$). Moreover, it is shown that the rth mode shape for viscous damping case is that for hysteretic damping case rotated by a constant phase angle which is -45° or 135° (or -225°). These features consist with the relationship between viscous damping and hysteretic damping models in non-proportional case concluded in Section 3.

Case No. 3: In a non-proportionally damped and close 3-dofs system, the localized hysteretic damping model is interpreted as a viscous damping model. The original system's stiffness and damping matrices are the same as those in Case No. 2 and the system's mass matrix is:

$$[M] = \begin{bmatrix} 1.0 & 0.0 & 0.0 \\ 0.0 & 0.95 & 0.0 \\ 0.0 & 0.0 & 1.05 \end{bmatrix}.$$

The mode shape matrix of this original system is:

$$[\Phi] = \begin{bmatrix} 0.578(-3.8^\circ) & 0.851(162.3^\circ) & 0.685(40.2^\circ) \\ 0.569(1.8^\circ) & 0.570(-101.5^\circ) & 1.020(176.0^\circ) \\ 0.588(2.0^\circ) & 0.848(11.6^\circ) & 0.560(-49.9^\circ) \end{bmatrix}.$$

The calculated $[A]$ and $[B]$ matrices can be obtained as:

$$[A] = \begin{bmatrix} 4.113 & 0.715 & 0.439 & 0.996 & 0.004 & 0.001 \\ 0.715 & 0.282 & 0.865 & 0.005 & 0.956 & -0.007 \\ 0.439 & 0.865 & 0.957 & 0.001 & -0.007 & 1.059 \\ 0.996 & 0.005 & 0.001 & 0.001 & 0.000 & 0.000 \\ 0.004 & 0.956 & -0.007 & 0.000 & -0.000 & -0.000 \\ 0.001 & -0.007 & 1.059 & 0.000 & -0.000 & -0.000 \end{bmatrix},$$

and

$$[B] = \begin{bmatrix} -2992 & 986 & 998 & -2.178 & -0.733 & -1.210 \\ 986 & -3021 & 1033 & -0.701 & 0.283 & 0.829 \\ 998 & 1033 & -3030 & 0.435 & 0.859 & 0.953 \\ -2.178 & 0.701 & 0.435 & 0.990 & 0.004 & -0.000 \\ -0.733 & 0.283 & 0.859 & 0.004 & 0.956 & -0.007 \\ -1.210 & 0.829 & 0.953 & -0.000 & -0.007 & 1.059 \end{bmatrix}.$$

The equivalent mode shape matrix is calculated as:

$$[\Psi] = \begin{bmatrix} 0.073(-48.8^\circ) & 0.076(-62.5^\circ) & 0.061(-4.5^\circ) \\ 0.071(-43.3^\circ) & 0.050(34.1^\circ) & 0.090(130.9^\circ) \\ 0.074(-43.0^\circ) & 0.076(146.5^\circ) & 0.050(-95.2^\circ) \end{bmatrix}.$$

The equivalent mass and stiffness matrices are only a little different from those of the original system in hysteretic damping case. And the relationship between the original and identified mode shape matrices can also be shown in this case by comparing the original and identified eigenvector matrices. Moreover, in this case, the equivalent damping matrix has no physical sense since it is not a positive-definite or semi-positive definite matrix. This can be verified by the following condition,

$$[\Psi]^H[C][\Psi] = [\Psi]^H \begin{bmatrix} 4.113 & 0.715 & 0.439 \\ 0.715 & 2.282 & 0.865 \\ 0.439 & 0.865 & 0.957 \end{bmatrix} [\Psi] = \begin{bmatrix} 0.05 & 0.017 - 0.003i & 0.01 + 0.01i \\ 0.017 + 0.003i & 0.023 & 0.009 + 0.013i \\ 0.01 - 0.01i & 0.009 - 0.013i & 0.009 \end{bmatrix}.$$

Case No. 4: In this case, a big and close mass–spring system, which has 8 dofs and is similar to the model shown in Fig. 1, is considered. It is also non-proportionally and hystereticly damped. The damping model is interpreted as a viscous damping model. The system's mass, stiffness and localized damping matrices are:

$$[M] = \begin{bmatrix} 1.0 & 0.0 & 0.0 & 0.0 & 0.0 & 0.0 & 0.0 & 0.0 \\ 0.0 & 1.0 & 0.0 & 0.0 & 0.0 & 0.0 & 0.0 & 0.0 \\ 0.0 & 0.0 & 1.0 & 0.0 & 0.0 & 0.0 & 0.0 & 0.0 \\ 0.0 & 0.0 & 0.0 & 1.0 & 0.0 & 0.0 & 0.0 & 0.0 \\ 0.0 & 0.0 & 0.0 & 0.0 & 1.0 & 0.0 & 0.0 & 0.0 \\ 0.0 & 0.0 & 0.0 & 0.0 & 0.0 & 1.0 & 0.0 & 0.0 \\ 0.0 & 0.0 & 0.0 & 0.0 & 0.0 & 0.0 & 1.0 & 0.0 \\ 0.0 & 0.0 & 0.0 & 0.0 & 0.0 & 0.0 & 0.0 & 1.0 \end{bmatrix},$$

$$
[K] = \begin{bmatrix} 2.0 & -1.0 & 0.0 & 0.0 & 0.0 & 0.0 & 0.0 & 0.0 \\ -1.0 & 2.0 & -1.0 & 0.0 & 0.0 & 0.0 & 0.0 & 0.0 \\ 0.0 & -1.0 & 2.0 & -1.0 & 0.0 & 0.0 & 0.0 & 0.0 \\ 0.0 & 0.0 & -1.0 & 2.0 & -1.0 & 0.0 & 0.0 & 0.0 \\ 0.0 & 0.0 & 0.0 & -1.0 & 2.0 & -1.0 & 0.0 & 0.0 \\ 0.0 & 0.0 & 0.0 & 0.0 & -1.0 & 2.0 & -1.0 & 0.0 \\ 0.0 & 0.0 & 0.0 & 0.0 & 0.0 & -1.0 & 2.0 & -1.0 \\ 0.0 & 0.0 & 0.0 & 0.0 & 0.0 & 0.0 & -1.0 & 2.0 \end{bmatrix},
$$

and

$$
[D] = \begin{bmatrix} 0.3 & 0.0 & 0.0 & 0.0 & 0.0 & 0.0 & 0.0 & 0.0 \\ 0.0 & 0.0 & 0.0 & 0.0 & 0.0 & 0.0 & 0.0 & 0.0 \\ 0.0 & 0.0 & 0.0 & 0.0 & 0.0 & 0.0 & 0.0 & 0.0 \\ 0.0 & 0.0 & 0.0 & 0.0 & 0.0 & 0.0 & 0.0 & 0.0 \\ 0.0 & 0.0 & 0.0 & 0.0 & 0.0 & 0.0 & 0.0 & 0.0 \\ 0.0 & 0.0 & 0.0 & 0.0 & 0.0 & 0.0 & 0.0 & 0.0 \\ 0.0 & 0.0 & 0.0 & 0.0 & 0.0 & 0.0 & 0.0 & 0.0 \\ 0.0 & 0.0 & 0.0 & 0.0 & 0.0 & 0.0 & 0.0 & 0.0 \end{bmatrix}.
$$

The mode shape matrix of the original system is:

$$
[\Phi] = \begin{bmatrix} 0.157(-13^\circ) & 0.301(169^\circ) & 0.414(-7^\circ) & 0.478(177^\circ) & 0.478(-177^\circ) & 0.158(-167^\circ) & 0.301(11^\circ) & 0.414(-173^\circ) \\ 0.299(-4^\circ) & 0.467(179^\circ) & 0.425(7^\circ) & 0.199(-148^\circ) & 0.199(32^\circ) & 0.299(4^\circ) & 0.467(-179^\circ) & 0.425(-7^\circ) \\ 0.407(-1^\circ) & 0.419(-175^\circ) & 0.082(82^\circ) & 0.415(-6^\circ) & 0.415(6^\circ) & 0.407(-179^\circ) & 0.419(-5^\circ) & 0.082(97^\circ) \\ 0.465(0^\circ) & 0.178(-164^\circ) & 0.408(176^\circ) & 0.315(11^\circ) & 0.315(169^\circ) & 0.465(-0^\circ) & 0.178(164^\circ) & 0.408(-176^\circ) \\ 0.467(1^\circ) & 0.159(-13^\circ) & 0.415(-176^\circ) & 0.306(171^\circ) & 0.306(-171^\circ) & 0.467(179^\circ) & 0.159(-167^\circ) & 0.415(-4^\circ) \\ 0.412(2^\circ) & 0.407(-1^\circ) & 0.041(97^\circ) & 0.410(-177^\circ) & 0.410(-3^\circ) & 0.412(-2^\circ) & 0.407(1^\circ) & 0.041(97^\circ) \\ 0.306(2^\circ) & 0.466(1^\circ) & 0.406(-1^\circ) & 0.162(-10^\circ) & 0.162(10^\circ) & 0.306(178^\circ) & 0.466(179^\circ) & 0.406(-179^\circ) \\ 0.163(3^\circ) & 0.305(2^\circ) & 0.409(1^\circ) & 0.463(1^\circ) & 0.463(179^\circ) & 0.163(-3^\circ) & 0.305(-2^\circ) & 0.409(-1^\circ) \end{bmatrix}.
$$

The calculated mass, stiffness and viscous damping matrices are:

$$
[M] = \begin{bmatrix} 0.988 & -0.004 & -0.004 & -0.003 & -0.002 & -0.001 & -0.001 & -0.000 \\ -0.004 & 0.998 & -0.003 & -0.002 & -0.001 & -0.001 & -0.000 & -0.000 \\ -0.004 & -0.003 & 0.998 & -0.002 & -0.001 & -0.001 & -0.000 & -0.000 \\ -0.003 & -0.002 & -0.002 & 0.999 & -0.001 & -0.001 & -0.000 & -0.000 \\ -0.002 & -0.001 & -0.001 & -0.001 & 1.000 & -0.001 & -0.001 & -0.000 \\ -0.001 & -0.001 & -0.001 & -0.001 & -0.001 & 1.000 & -0.001 & -0.001 \\ -0.001 & -0.000 & -0.000 & -0.000 & -0.001 & -0.001 & 1.000 & -0.001 \\ -0.000 & -0.000 & -0.000 & -0.000 & -0.000 & -0.001 & -0.001 & 1.0 \end{bmatrix},
$$

$$[K]=\begin{bmatrix} 2.03 & -1.00 & 0.00 & 0.00 & 0.00 & 0.00 & 0.00 & 0.00 \\ -1.00 & 2.00 & -1.00 & -0.00 & 0.00 & 0.00 & 0.00 & 0.00 \\ 0.00 & -1.00 & 2.00 & -1.00 & -0.00 & 0.00 & 0.00 & 0.00 \\ 0.00 & -0.00 & -1.00 & 2.00 & -1.00 & -0.00 & 0.00 & 0.00 \\ 0.00 & 0.00 & -0.00 & -1.00 & 2.00 & -1.00 & -0.00 & 0.00 \\ 0.00 & 0.00 & 0.00 & -0.00 & -1.00 & 2.00 & -1.00 & -0.00 \\ 0.00 & 0.00 & 0.00 & 0.00 & -0.00 & -1.00 & 2.00 & -1.00 \\ 0.00 & 0.00 & 0.00 & 0.00 & 0.000 & -0.00 & -1.00 & 2.00 \end{bmatrix},$$

and

$$[C]=\begin{bmatrix} 0.137 & 0.024 & 0.002 & 0.002 & 0.002 & 0.001 & 0.000 & 0.000 \\ 0.024 & 0.019 & 0.006 & -0.003 & -0.000 & 0.000 & 0.000 & 0.000 \\ 0.002 & 0.006 & 0.015 & 0.004 & -0.004 & -0.001 & 0.000 & 0.000 \\ 0.002 & -0.003 & 0.004 & 0.014 & 0.003 & -0.005 & -0.001 & -0.000 \\ 0.001 & -0.000 & -0.004 & 0.003 & 0.014 & 0.003 & -0.005 & -0.001 \\ 0.001 & 0.000 & -0.001 & -0.005 & 0.003 & 0.014 & 0.003 & -0.005 \\ 0.000 & 0.000 & 0.000 & -0.001 & -0.005 & 0.003 & 0.014 & 0.004 \\ 0.000 & 0.000 & 0.000 & -0.000 & -0.001 & -0.005 & 0.004 & 0.019 \end{bmatrix}.$$

The equivalent mode shape matrix is:

$$[\Psi]=\begin{bmatrix} 0.190(-58^\circ) & 0.258(-56^\circ) & 0.294(-52^\circ) & 0.298(-48^\circ) & 0.273(-42^\circ) & 0.079(-32^\circ) & 0.155(-34^\circ) & 0.222(-38^\circ) \\ 0.359(-49^\circ) & 0.399(-46^\circ) & 0.299(-38^\circ) & 0.123(-13^\circ) & 0.115(104^\circ) & 0.151(139^\circ) & 0.241(136^\circ) & 0.229(128^\circ) \\ 0.487(-46^\circ) & 0.357(-40^\circ) & 0.058(39^\circ) & 0.254(129^\circ) & 0.237(141^\circ) & 0.205(-44^\circ) & 0.216(-50^\circ) & 0.044(-127^\circ) \\ 0.557(-45^\circ) & 0.150(-29^\circ) & 0.289(131^\circ) & 0.195(146^\circ) & 0.180(-56^\circ) & 0.234(135^\circ) & 0.092(119^\circ) & 0.219(-41^\circ) \\ 0.559(-44^\circ) & 0.136(122^\circ) & 0.292(139^\circ) & 0.191(-54^\circ) & 0.174(-36^\circ) & 0.235(-46^\circ) & 0.082(148^\circ) & 0.223(131^\circ) \\ 0.492(-43^\circ) & 0.347(134^\circ) & 0.029(-141^\circ) & 0.255(-42^\circ) & 0.235(132^\circ) & 0.208(133^\circ) & 0.210(-44^\circ) & 0.022(-127^\circ) \\ 0.366(-43^\circ) & 0.397(136^\circ) & 0.287(-46^\circ) & 0.101(-125^\circ) & 0.092(145^\circ) & 0.154(-47^\circ) & 0.240(134^\circ) & 0.218(-44^\circ) \\ 0.195(-43^\circ) & 0.260(137^\circ) & 0.288(-44^\circ) & 0.288(136^\circ) & 0.264(46^\circ) & 0.082(132^\circ) & 0.157(-47^\circ) & 0.220(136^\circ) \end{bmatrix}.$$

Case No. 5: In a proportionally damped 3-dofs system, the distributed viscous damping model is interpreted as a hysteretic damping model. The system's stiffness matrix is as that in Case No. 1, and the mass and viscous damping matrices are:

$$[M]=\begin{bmatrix} 1.0 & 0.0 & 0.0 \\ 0.0 & 0.95 & 0.0 \\ 0.0 & 0.0 & 1.05 \end{bmatrix} \quad \text{and} \quad [C]=\begin{bmatrix} 4.8 & -1.6 & -1.6 \\ -1.6 & 4.8 & -1.6 \\ -1.6 & -1.6 & 4.8 \end{bmatrix}.$$

The original system's mode shape matrix is:

$$[\Psi]=\begin{bmatrix} 0.073(-45^\circ) & 0.054(-45^\circ) & 0.049(-45^\circ) \\ 0.071(-45^\circ) & 0.019(-45^\circ) & 0.073(135^\circ) \\ 0.074(-45^\circ) & 0.067(135^\circ) & 0.018(-45^\circ) \end{bmatrix}.$$

The calculated mass, stiffness, and hysteretic damping matrices are:

$$[M]=\begin{bmatrix}1.00 & 0.00 & 0.00\\ 0.00 & 0.95 & 0.00\\ 0.00 & 0.00 & 1.05\end{bmatrix},\quad [K]=\begin{bmatrix}3000 & -1000 & -1000\\ -1000 & 3000 & -1000\\ -1000 & -1000 & 3000\end{bmatrix}\quad \text{and}\quad [D]=\begin{bmatrix}287 & -120 & -116\\ -120 & 293 & -118\\ -116 & -118 & 281\end{bmatrix}.$$

The equivalent mode shape matrix is obtained as:

$$[\Phi]=\begin{bmatrix}0.577 & 0.602 & 0.552\\ 0.567 & 0.215 & -0.827\\ 0.586 & -0.752 & 0.207\end{bmatrix}.$$

In this case, the equivalent mass and stiffness matrices are the same as those of the original system. In addition, the equivalent damping matrix $[D]$ is demonstrated to be physically sensible.

Case No. 6: In a 3-dofs close system with non-proportional viscous damping, the damping model is interpreted as a hysteretic damping model. The system's mass and stiffness matrices are same as those in Case No. 5. The original localized viscous damping and mode shape matrices are as follows:

$$[C]=\begin{bmatrix}9.6 & 0.0 & 0.0\\ 0.0 & 0.0 & 0.0\\ 0.0 & 0.0 & 0.0\end{bmatrix},$$

$$[\Psi]=\begin{bmatrix}0.077(-42^\circ) & 0.023(39^\circ) & 0.073(-49^\circ)\\ 0.042(96^\circ) & 0.074(143^\circ) & 0.072(-43^\circ)\\ 0.045(152^\circ) & 0.059(-57^\circ) & 0.074(-43^\circ)\end{bmatrix}.$$

The calculated mass, stiffness and hysteretic damping matrices are:

$$[M]=\begin{bmatrix}0.996 & -0.019 & 0.013\\ -0.019 & 0.963 & 0.006\\ 0.013 & 0.006 & 1.033\end{bmatrix},\quad [K]=\begin{bmatrix}2996 & -1070 & -944\\ -1070 & 3052 & -978\\ -944 & -978 & 2930\end{bmatrix}\quad \text{and}\quad [D]=\begin{bmatrix}391 & -63 & -88\\ -63 & 33 & 51\\ -88 & 51 & 79\end{bmatrix}.$$

The equivalent mode shape matrix is identified as:

$$[\Phi]=\begin{bmatrix}0.862(3^\circ) & 0.264(84^\circ) & 0.580(-4^\circ)\\ 0.465(140^\circ) & 0.837(187^\circ) & 0.571(2^\circ)\\ 0.505(-164^\circ) & 0.669(-13^\circ) & 0.590(2^\circ)\end{bmatrix}.$$

Case No. 7: A big and close mass–spring system, which is non-proportionally and viscously damped, is considered in this case. The system's mass and stiffness matrices are the same as those in Case No. 4. A hysteretic damping model is assumed for the system incorrectly. The system has damping at two locations apart from each other so that the damping matrix is localized as:

$$[C]=\begin{bmatrix}0.3 & 0.0 & 0.0 & 0.0 & 0.0 & 0.0 & 0.0 & 0.0\\ 0.0 & 0.0 & 0.0 & 0.0 & 0.0 & 0.0 & 0.0 & 0.0\\ 0.0 & 0.0 & 0.0 & 0.0 & 0.0 & 0.0 & 0.0 & 0.0\\ 0.0 & 0.0 & 0.0 & 0.0 & 0.0 & 0.0 & 0.0 & 0.0\\ 0.0 & 0.0 & 0.0 & 0.0 & 0.0 & 0.0 & 0.0 & 0.0\\ 0.0 & 0.0 & 0.0 & 0.0 & 0.0 & 0.0 & 0.0 & 0.0\\ 0.0 & 0.0 & 0.0 & 0.0 & 0.0 & 0.0 & 0.0 & 0.0\\ 0.0 & 0.0 & 0.0 & 0.0 & 0.0 & 0.0 & 0.0 & 0.3\end{bmatrix}.$$

The mode shape matrix of the original system is:

$$[\Psi]=\begin{bmatrix} 0.193(-49^\circ) & 0.260(-51^\circ) & 0.294(-51^\circ) & 0.300(-47^\circ) & 0.276(-41^\circ) & 0.224(-34^\circ) & 0.154(28^\circ) & 0.077(-24^\circ)\\ 0.364(-46^\circ) & 0.399(-45^\circ) & 0.294(-39^\circ) & 0.118(-14^\circ) & 0.119(102^\circ) & 0.232(126^\circ) & 0.243(135^\circ) & 0.150(139^\circ)\\ 0.490(-45^\circ) & 0.351(-43^\circ) & 0.029(42^\circ) & 0.255(131^\circ) & 0.230(139^\circ) & 0.038(-124^\circ) & 0.219(-51^\circ) & 0.208(-46^\circ)\\ 0.558(-44^\circ) & 0.139(-42^\circ) & 0.288(135^\circ) & 0.187(138^\circ) & 0.172(-49^\circ) & 0.216(-46^\circ) & 0.087(127^\circ) & 0.239(132^\circ)\\ 0.558(-44^\circ) & 0.139(138^\circ) & 0.288(135^\circ) & 0.187(-42^\circ) & 0.172(-49^\circ) & 0.216(134^\circ) & 0.087(127^\circ) & 0.239(-48^\circ)\\ 0.490(-45^\circ) & 0.351(137^\circ) & 0.029(42^\circ) & 0.255(-49^\circ) & 0.230(139^\circ) & 0.038(56^\circ) & 0.219(-51^\circ) & 0.208(134^\circ)\\ 0.364(-46^\circ) & 0.399(135^\circ) & 0.294(-39^\circ) & 0.118(166^\circ) & 0.119(102^\circ) & 0.232(-54^\circ) & 0.243(134^\circ) & 0.150(-41^\circ)\\ 0.194(-49^\circ) & 0.260(129^\circ) & 0.294(-51^\circ) & 0.300(133^\circ) & 0.276(-41^\circ) & 0.223(146^\circ) & 0.154(-28^\circ) & 0.077(-156^\circ) \end{bmatrix}.$$

The calculated mass, stiffness and viscous damping matrices are:

$$[M]=\begin{bmatrix} 0.994 & -0.006 & -0.000 & -0.002 & -0.000 & 0.000 & -0.000 & -0.000\\ -0.006 & 0.999 & 0.003 & 0.000 & -0.002 & -0.000 & 0.000 & -0.000\\ -0.001 & 0.003 & 0.998 & 0.002 & 0.001 & -0.002 & -0.000 & 0.000\\ -0.003 & 0.000 & 0.002 & 0.999 & 0.002 & 0.001 & -0.002 & -0.000\\ -0.000 & -0.002 & 0.001 & 0.002 & 0.999 & 0.002 & 0.000 & -0.003\\ 0.000 & -0.000 & -0.002 & 0.001 & 0.002 & 0.998 & 0.003 & -0.001\\ -0.000 & 0.000 & -0.000 & -0.002 & 0.000 & 0.003 & 0.999 & -0.006\\ -0.000 & -0.000 & 0.000 & -0.000 & -0.003 & -0.001 & -0.006 & 0.994 \end{bmatrix},$$

$$[K]=\begin{bmatrix} 1.995 & -1.007 & 0.002 & -0.003 & 0.002 & 0.001 & -0.000 & -0.000\\ -1.007 & 2.000 & -0.994 & 0.001 & -0.005 & 0.002 & 0.001 & -0.000\\ 0.002 & -0.994 & 1.992 & -0.995 & 0.002 & -0.006 & 0.002 & 0.001\\ -0.003 & 0.001 & -0.995 & 1.993 & -0.995 & 0.002 & -0.005 & 0.002\\ 0.002 & -0.005 & 0.002 & -0.995 & 1.993 & -0.995 & 0.001 & -0.003\\ 0.001 & 0.002 & -0.006 & 0.002 & -0.995 & 1.992 & -0.994 & 0.002\\ -0.000 & 0.001 & 0.002 & -0.005 & 0.001 & -0.994 & 2.000 & -1.007\\ -0.000 & -0.000 & 0.001 & 0.002 & -0.003 & 0.002 & -1.007 & 1.995 \end{bmatrix},$$

and

$$[D]=\begin{bmatrix} 0.263 & -0.039 & -0.037 & -0.001 & -0.000 & -0.002 & -0.001 & -0.000\\ -0.039 & 0.042 & 0.000 & -0.021 & 0.005 & 0.002 & -0.000 & -0.000\\ -0.037 & 0.000 & 0.041 & -0.005 & -0.023 & 0.005 & 0.002 & -0.002\\ -0.001 & -0.021 & -0.005 & 0.042 & -0.005 & -0.023 & 0.005 & -0.000\\ -0.000 & 0.005 & -0.023 & -0.005 & 0.041 & -0.005 & -0.021 & -0.001\\ -0.002 & 0.002 & 0.005 & -0.023 & -0.005 & 0.041 & 0.000 & -0.037\\ -0.001 & -0.000 & 0.002 & 0.005 & -0.021 & 0.000 & 0.042 & -0.039\\ -0.000 & -0.000 & -0.002 & -0.000 & -0.001 & -0.037 & -0.039 & 0.263 \end{bmatrix}.$$

The equivalent mode shape matrix is:

$$[\Psi]=\begin{bmatrix}0.161(-4^\circ) & 0.304(-6^\circ) & 0.415(-6^\circ) & 0.480(-2^\circ) & 0.483(4^\circ) & 0.417(10^\circ) & 0.298(17^\circ) & 0.153(21^\circ)\\ 0.303(-1^\circ) & 0.467(0^\circ) & 0.419(6^\circ) & 0.194(30^\circ) & 0.203(146^\circ) & 0.430(171^\circ) & 0.469(180^\circ) & 0.298(-176^\circ)\\ 0.409(0^\circ) & 0.412(2^\circ) & 0.042(84^\circ) & 0.407(176^\circ) & 0.404(-176^\circ) & 0.069(-79^\circ) & 0.423(-6^\circ) & 0.412(-1^\circ)\\ 0.465(1^\circ) & 0.163(3^\circ) & 0.408(-180^\circ) & 0.301(-176^\circ) & 0.299(-4^\circ) & 0.401(0^\circ) & 0.169(172^\circ) & 0.474(177^\circ)\\ 0.465(1^\circ) & 0.163(-177^\circ) & 0.408(-180^\circ) & 0.301(3^\circ) & 0.299(-4^\circ) & 0.401(180^\circ) & 0.169(172^\circ) & 0.474(-3^\circ)\\ 0.409(0^\circ) & 0.412(-178^\circ) & 0.042(84^\circ) & 0.407(-4^\circ) & 0.404(-176^\circ) & 0.069(100^\circ) & 0.423(-6^\circ) & 0.412(179^\circ)\\ 0.303(-1^\circ) & 0.467(-180^\circ) & 0.419(6^\circ) & 0.194(-150^\circ) & 0.203(146^\circ) & 0.430(-9^\circ) & 0.469(180^\circ) & 0.298(4^\circ)\\ 0.161(-4^\circ) & 0.304(174^\circ) & 0.415(-6^\circ) & 0.480(178^\circ) & 0.483(4^\circ) & 0.417(-170^\circ) & 0.298(17^\circ) & 0.153(-159^\circ)\end{bmatrix}.$$

Case Nos. 1 and 5 are the cases in which the damping matrices (hysteretic and viscous) are proportional. Therefore, an exact relationship between hysteretic and viscous damping models exists in these two cases since no assumption has been made for the proportional damping case. The equivalent damping matrix is no longer proportional (cannot be expressed as a linear combination of $[M]$ and $[K]$) while the system still has real modes. Moreover, the identified damping models are physically sensible in the case of distributed damping properties. Case No. 2 is the case where a non-proportional damping system has well separated modes. In this case, the estimation errors between the original mass and stiffness matrices and the calculated ones are very small, but the calculated damping matrix is no longer physically sensible since damping properties are localized. Case Nos. 3 and 6 are closely coupled systems with damping being localized. In these two cases, the mode shapes of the original system and its equivalent counterparts are effectively the same except differing by a complex scaling factor. Moreover, as in Case No. 2, the equivalent damping matrices are not physically meaningful. The errors between the original system's mass, stiffness and the calculated ones are also quite small ($<5\%$). In order to demonstrate whether the theory is valid for large systems, Case No. 4 and Case No. 7, where an 8-dofs system with non-proportional damping is presented, were also studied. The difference between these two cases is that Case No. 7 has the localized damping properties at two separated locations. The similar numerical results to the calculated ones from Case No. 3 were also obtained for Case No. 4. So were the calculated results from Case No. 7 compared with those from Case No. 6. However, the calculated equivalent damping matrices in the two cases would not possess physical meanings any more. All these shows the above derived theory can be extended to various much larger systems with confidence.

The above various simulated case studies have verified that the mode shapes obtained from arbitrary interpretation of modal data are accurate enough to be used to modify the analytical FE model. Moreover, the identified special model including mass and stiffness matrices is consistent with those of the original system. However, if the damping information of a system is sought and the damping of the system is localized, then the correct interpretation of damping model becomes very important. Because, in this case there is no physically sensible equivalent damping matrix existing.

6. Experimental case study

To highlight the significance of interpreting damping model for a damped mechanical system, a sample experimental case study was conducted. This case study is based on the experimental modal testing of a beam. The sketch of the experiment set up is shown as Fig. 2, in which a test aluminum beam is free–free suspended. The lateral responses (in y direction) were measured by an accelerometer at the nine measurement points on the beam with the hammer excitation at the sixth point in y direction. And then the FRF data were gathered from the FFT analyzer and transferred into the computer. Subsequently, the modal analysis procedure was performed using the ICATS software to extract modal parameters, such as nature frequencies, modal shapes and damping loss factors.

The typical measured FRFs, where five resonant peaks are observed, are shown in Fig. 3 and the identified modal data for the first five modes are list in Table 1 except the mode shapes. The mode shape matrix of this

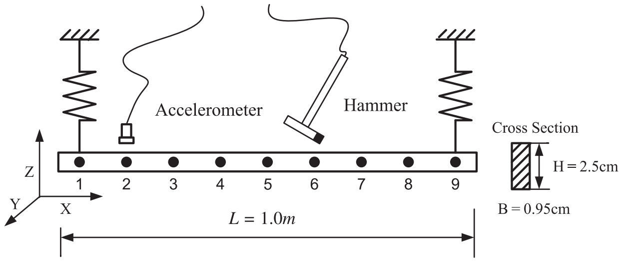

Fig. 2. The measure sketch of a free–free beam.

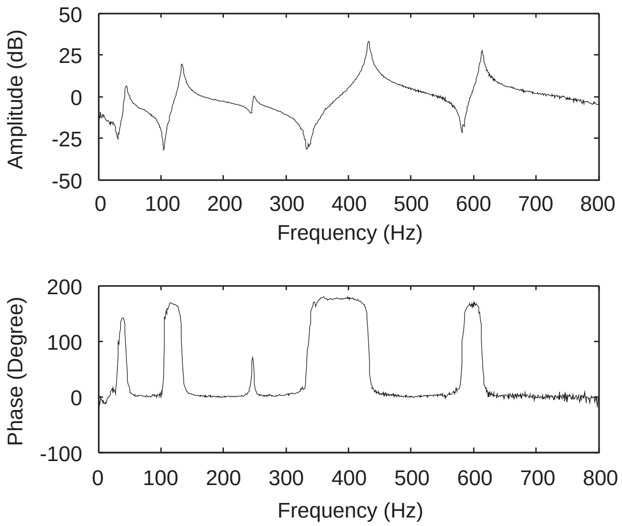

Fig. 3. The typical FRF measured at the 4th measurement point.

Table 1
The identified natural frequencies and damping loss factors of the beam (hysteretic damping).

Mode no. (r)	1	2	3	4	5
Natural frequency f_r (Hz)	44.5	134.0	247.4	432.8	612.7
Natural frequency ω_r (rad/s)	279.6	842.0	1554.5	2719.4	3849.7
Damping loss factor (η_r)	0.0967	0.0287	0.0171	0.0092	0.0070
Damping ratio (ξ_r) (viscous damping)	0.0484	0.0143	0.0086	0.0046	0.0035

damped structure is obtained as:

$$[\Phi] = \begin{bmatrix} 1.009(86.4^\circ) & 0.792(13.6^\circ) & 0.799(102^\circ) & 0.906(178^\circ) & 0.635(-89.3^\circ) \\ 0.388(93.1^\circ) & 0.036(-171^\circ) & 0.247(-28.3^\circ) & 0.540(-6.4^\circ) & 0.626(82.9^\circ) \\ 0.105(-90.3^\circ) & 0.599(-173^\circ) & 0.588(-83.8^\circ) & 0.180(6.4^\circ) & 0.229(-111^\circ) \\ 0.577(-83.5^\circ) & 0.542(175^\circ) & 0.115(98.9^\circ) & 0.590(-179^\circ) & 0.438(-107^\circ) \\ 0.804(-77.6^\circ) & 0.004(169^\circ) & 0.392(146^\circ) & 0.006(3.9^\circ) & 0.699(97.0^\circ) \\ 0.396(-88.7^\circ) & 0.485(-1.3^\circ) & 0.129(88.8^\circ) & 0.631(3.9^\circ) & 0.420(-82.5^\circ) \\ 0.135(-90.5^\circ) & 0.629(4.5^\circ) & 0.512(-77.7^\circ) & 0.140(-170^\circ) & 0.363(-86.2^\circ) \\ 0.369(91.8^\circ) & 0.059(1.5^\circ) & 0.225(-97.9^\circ) & 0.545(176^\circ) & 0.581(75.6^\circ) \\ 0.988(82.2^\circ) & 0.807(177^\circ) & 0.603(89.6^\circ) & 0.699(30.3^\circ) & 0.654(-94.0^\circ) \end{bmatrix}.$$

It can be observed from the identified mode shape matrix that the structural system is close to a proportionally damping system though some phase angels seem not to agree well with it due to the estimation errors.

In this case, the modal parameters were estimated based on the response function model, in which hysteretic damping is involved. In fact, the hysteretic damping model can be assumed confidently for this beam since the beam is uniformly made of aluminum and only the hysteresis properties of material in the structure needs to be considered for the damping model. Hence, the hysteretic damping matrix of the beam structure is established as:

$$[D] = \begin{bmatrix} 1.924\text{e}5 & 5.069\text{e}6 & -2.177\text{e}7 & -1.565\text{e}7 & -1.270\text{e}7 \\ -4.400\text{e}6 & 6.348\text{e}5 & -4.564\text{e}7 & -3.247\text{e}7 & -2.476\text{e}7 \\ 2.218\text{e}7 & 4.628\text{e}7 & 5.175\text{e}5 & 4.305\text{e}6 & -2.651\text{e}6 \\ 1.584\text{e}7 & 3.281\text{e}7 & -3.548\text{e}6 & 4.186\text{e}5 & -2.823\text{e}6 \\ 1.277\text{e}7 & 2.487\text{e}7 & 3.152\text{e}6 & 3.348\text{e}6 & 1.881\text{e}5 \end{bmatrix}.$$

Here, it should be noted that the damping model is a 5×5 matrix since the identified modes are incomplete compared with the measured points (or coordinate) in this experiment.

Provided that the viscous damping model is adopted for the structural system, a little different modal data may be identified according to the modal analysis procedure from hysteretic damping model to viscous damping model indicated in Section 3. The identified undamped natural frequencies in this case are as same as those in the case of hysteretic damping. Moreover, the damping ratios for viscous damping shown in Table 1 have the values as $\xi_r = \eta_r/2$ ($r = 1,2,\ldots,5$). The calculated equivalent mode shape matrix in the case of viscous damping is as follows:

$$[\Psi] = \begin{bmatrix} 0.047(-139^\circ) & 0.019(-31.3^\circ) & 0.015(56.9^\circ) & 0.012(133^\circ) & 0.007(45.7^\circ) \\ 0.016(-132^\circ) & 0.001(144^\circ) & 0.004(-72.9^\circ) & 0.007(-51.4^\circ) & 0.007(-142^\circ) \\ 0.004(44.7^\circ) & 0.015(142^\circ) & 0.011(-129^\circ) & 0.002(-38.6^\circ) & 0.003(23.3^\circ) \\ 0.024(51.5^\circ) & 0.013(130^\circ) & 0.002(54.0^\circ) & 0.008(136^\circ) & 0.005(27.4^\circ) \\ 0.034(57.6^\circ) & 0.000(124^\circ) & 0.007(101^\circ) & 0.000(-41.1^\circ) & 0.008(-128^\circ) \\ 0.017(46.2^\circ) & 0.012(-46.3^\circ) & 0.002(43.8^\circ) & 0.009(-41.1^\circ) & 0.005(52.5^\circ) \\ 0.006(44.5^\circ) & 0.015(-40.5^\circ) & 0.009(-123^\circ) & 0.002(145^\circ) & 0.004(48.8^\circ) \\ 0.016(-133^\circ) & 0.001(-43.5^\circ) & 0.004(-143^\circ) & 0.007(131^\circ) & 0.007(-149^\circ) \\ 0.042(-143^\circ) & 0.020(132^\circ) & 0.011(44.6^\circ) & 0.009(-14.7^\circ) & 0.007(41.0^\circ) \end{bmatrix}.$$

It can be found that these eigenvectors are effectively same as those identified in the case of hysteretic damping except differing by a complex scaling factor, the matrix of which can be written after calculation as,

$$[N] = \begin{bmatrix} 0.042(135^\circ) & 0 & 0 & 0 & 0 \\ 0 & 0.024(-45^\circ) & 0 & 0 & 0 \\ 0 & 0 & 0.018(-45^\circ) & 0 & 0 \\ 0 & 0 & 0 & 0.014(135^\circ) & 0 \\ 0 & 0 & 0 & 0 & 0.011(135^\circ) \end{bmatrix}.$$

From the complex matrix $[N]$, it is observed that the modulus of the diagonal element for the rth ($r = 1,2,\ldots,5$) mode shape is equal to $1/\sqrt{2\omega_r}$ ($r = 1,2,\ldots,5$). In addition, the rth mode shape for viscous damping case is that for hysteretic damping case rotated by a constant phase angle which is -45° or 135°. Based on the identified modal data for viscous damping case, the viscous damping matrices is produced as,

$$[C] = \begin{bmatrix} 9.828e5 & 2.285e6 & 7.152e5 & 7.406e5 & -0.524e5 \\ 2.285e6 & 5.315e6 & 1.664e6 & 1.725e6 & -1.209e5 \\ 7.152e5 & 1.664e6 & 5.185e5 & 5.384e5 & -0.3938e5 \\ 7.406e5 & 1.727e6 & 5.384e5 & 5.618e5 & -0.389e5 \\ -0.524e5 & -1.209e5 & -0.393e5 & -0.389e5 & 0.024e5 \end{bmatrix}.$$

In addition, the calculated damping matrix for viscous case has no physical meanings. As can be seen, these results from the experimental test have sufficiently demonstrated the relationship between viscous damping and hysteretic damping models in non-proportional case, which has been derived previously.

7. Concluding remarks

In this paper, to address the effect of a reasonable damping model on estimated modal parameters, the authors have investigated the relation of the modal models for viscous and hysteretic damping cases in detail. And the certain relationship between the two damping models has been presented based on the normalization procedures and the corresponding modal analysis procedures. In the case of a proportionally damped system, there exists an exact relationship between hysteretic and viscous damping models as $\eta_r = 2\xi_r$. The derived mass and stiffness matrices are the same as those of the original system. The calculated damping matrix is still real though not proportional. As for a non-proportionally damped system, the equivalent mode shapes and their counterparts of the original system are almost the same except differing by a complex scaling factor, and the errors between the original mass, stiffness matrices and the calculated ones are quit small. Numerical cases have shown sufficiently that the error in the estimation of modal parameters caused by the wrong selection of damping model is really quite small since the original and calculated systems with different damping models have the same response model. Moreover, the equivalent damping matrix is physically sensible in the case of the system with distributed damping. Whereas, if the damping is localized, the correct interpretation becomes very important since no physically sensible equivalent damping matrix exists in this case. The experimental example based on a sample vibration test has further demonstrated the validity of the investigation on the relationship between the two damping models.

References

[1] L. Rayleigh, *Theory of Sound (two volumes)*, second edition, Dover Publications, New York, 1897 1945 re-issue.
[2] T.K. Caughey, Classical normal modes in damped linear dynamic systems, *Journal of Applied Mechanics* 27 (1960) 269–271.
[3] T.K. Caughey, M.E.J. O'Kelly, Classical normal modes in damped linear dynamic systems, *Transactions of ASME, Journal of Applied Mechanics* 32 (1965) 583–588.
[4] D.J. Ewins, *Modal Testing: Theory, Practice and Application*, second ed., Research Studies Press, UK, 2000.
[5] N.M.M. Maia, J.M.M. Silva, *Theoretical and Experimental Modal Analysis*, John Wiley & Sons Inc., New York, 1997.
[6] S.R. Ibrahim, Computation of normal modes from identified complex modes, *AIAA Journal* 21 (3) (1983) 446–451.
[7] C. Lin, S.R. Ibrahim, The use of complex versus normal modes in structural model improvement, *Proceedings of the Second IMAC*, 1984, pp. 415–424.
[8] S.Y. Chen, M.S. Ju, Y.G. Tsuei, Extraction of normal modes for highly coupled incomplete systems with general damping, *Mechanical Systems and Signal Processing* 10 (1) (1996) 93–106.
[9] S. Adhikari, Damping modelling using generalized proportional damping, *Journal of Sound and Vibration* 293 (2006) 156–170.
[10] M.E. Gaylard, Identification of proportional and other sorts of damping matrices using a weighted response-integral method, *Mechanical Systems and Signal Processing* 15 (2) (2001) 245–256.
[11] J. Angeles, S. Ostrovskaya, The proportional-damping matrix of arbitrarily damped linear mechanical systems, *Transactions of the ASME, Journal of Applied Mechanics* 69 (2002) 649–656.
[12] C. Minas, D.J. Inman, Identification of a nonproportional damping matrix from incomplete modal information, *ASME Journal of Vibration and Acoustics* 113 (1991) 219–224.
[13] M. Tong, Z. Liang, G.C. Lee, *Proceedings of 10th IMAC, on the Non-proportionality of Generally Damped Systems*, 1992, pp.1302–1308.

[14] K. Liu, M.R. Kujath, W.P. Zheng, Evaluation of damping non-proportionality using identified modal information, *Mechanical Systems and Signal Processing* 15 (1) (2001) 227–242.

[15] W. Gawronski, J.T. Sawicki, Response errors of non-proportionally lightly damped structures, *Journal of Sound and Vibration* 200 (1997) 543–550.

[16] J. Woodhouse, Linear damping models for structural vibration, *Journal of Sound and Vibration* 215 (3) (1998) 547–569.

[17] S. Adhikari, J. Woodhouse, Identification of damping: part 1, viscous damping, *Journal of Sound and Vibration* 243 (1) (2001) 43–61.

[18] S. Adhikari, J. Woodhouse, Identification of damping: part 2, non-viscous damping, *Journal of Sound and Vibration* 243 (1) (2001) 63–88.

[19] U. Prells, M.I. Friswell, A measure of non-proportional damping, *Mechanical Systems and Signal Processing* 14 (2) (2000) 125–137.

[20] T. Kasai, M. Link, Identification of non-proportional modal damping matrix and real normal modes, *Mechanical Systems and Signal Processing* 16 (6) (2002) 921–934.

[21] E. Balmés, New results on the identification of normal modes from experimental complex modes, *Mechanical Systems and Signal Processing* 11 (2) (1997) 229–243.

[22] R.M. Lin, Identification of the Dynamic Characteristics of Nonlinear Structures, PhD Thesis, Imperial College of Science, Technology and Medicine, London, UK, 1990.